

# Investigation of the Thermal Behaviour in the Lubricating Gap of an Axial Piston Pump with Respect to Lifetime

Roman Ivantysyn, Prof. Dr. Jürgen Weber

TU Dresden, Institute of Fluid Power (IFD), Helmholtzstr. 7a, D-01062 Dresden, Germany  
E-Mail: ivanty@mx.tu-dresden.de, fluidtronik@mailbox.tu-dresden.de

Axial piston pumps are universal displacement machines that are used in a vast variety of applications. Their high pressure resistance and ease of operation make them very popular, especially in mobile applications and aerospace. The lifetime of axial piston pumps is depending on the design of the rotating kit, the application and its overall robustness to external loads. The fluid film between the moving parts is responsible for bearing the loads and sealing the displacement chambers. Its design is the most complicated part for a pump designer. All pumps to this date have been designed in a trial and error process, which is not only costly, but doesn't yield an optimum in terms of efficiency and robustness. This paper aims to investigate the influence the fluid film has on the lifetime of the pump. From the three main lubricating interfaces of an axial piston pump, two - cylinder block / valve plate and slipper / swash plate - were analysed in terms of temperature for both interfaces and gap height for slipper only by means of measurements and simulation. The simulation tool that was used for the analysis is called Caspar FSTI, developed by Purdue University. It is capable of calculating the resulting gap height between all three main interfaces resulting from force balance calculations between external and fluid film forces due to the pressure distribution in the gap and taking both deformation due to temperature and pressure into account. The simulation will be used to understand the behaviour of the pump while the measurements will give a deeper look into the actual steady state conditions as well as transient behaviour of the parts including wear in.

**Keywords:** Axial Piston Machines, Lifetime, Lubricating Gap Design, Temperature Field  
**Target audience:** Mobile Hydraulics, Mining Industry, Component Design, Design Process

## 1 Introduction

Axial piston pumps are positive displacement machines that are used in a vast variety of applications. Their high pressure resistance and ease of operation make them very popular, especially in heavy duty applications. Some applications require more robust pumps with an extended lifetime, particularly those that operate in remote environments such as the marine type or mining operations.

To understand the physical phenomena that can cause premature failure, it is necessary to take a closer look on the sealing gaps in these positive displacement machines. The lubricating gaps in piston pumps are the primary source of the power losses and also produce particles due to wear. These gaps have been in the focus of many researches over the last 30 years [1, 2, 3]. In the last 15 years vast improvements in the computational power have paved the way to more complex simulation models of these lubricating gaps [4, 5, 6, 7, 8]. One particular simulation model, Caspar FSTI, has proven itself to be a highly reliably and capable model for swash plate type axial piston pumps [5, 6, 7]. The model predicts the lubricating film thickness in all major lubricating gaps and considers all major physical effects such as deformation of the parts due to temperature and pressure. This simulation model was used in this research to evaluate the pump before any measurements were done, in order to place the sensors at the right locations, as well as to understand the measured phenomena including the gap height. The authors published two previous publications, validating the software for both interfaces [9, 10].

For this research, a unique test stand has been developed, which is capable of measuring fluid film thickness using eddy current gap height sensors, while simultaneously measuring temperature using thermocouples, which

were placed directly in the sealing interface of the valve plate and the swash plate (see Figure 3). Previous researchers have measured gap height or temperature in these interfaces before [6, 7, 8, 11, 12]. However, none have measured both the temperature and the fluid film thickness at the same time, and none have looked at two interfaces simultaneously. The two most noteworthy were Zecchi [7] and Schenk [6]. Zecchi placed 22 thermocouples directly underneath the running surface of the valve plate and used it to validate his research work, which ended up being the cylinder block/valve plate model in Caspar FSTI. The slipper/swash plate model of Caspar was developed by Schenk, who validated his model using fluid film measurements using eddy current mounted in the swash plate, measuring the gap to the slippers across the entire shaft rotation.

Building on all of this prior work, the "transparent pump" test stand was developed, which enables a deeper look into the inner workings of an axial piston pump. The goal of this paper is aimed to show how the pump reacts to different operating conditions both in transient and stationary form, as well as how the wear-in can change the pumps behaviour. This was determined using measurements and simulation. In this paper, the measurement results will be in the primary focus.

## 2 Research goal and approach

As described in the introduction, there are many publications that performed research in the area of lubricating gaps within piston pumps. The goal of this research is to build on those and develop a holistic approach for the lifetime prediction and eventually life time extension of axial piston pumps. In order to achieve this, the lifetime limiting factors such as wear, were observed during measurements and analysed using different parameters such as temperature and particle generation. As already described, this paper focuses on two of the three main interfaces of axial piston pumps, as shown in yellow and red in Figure 1.

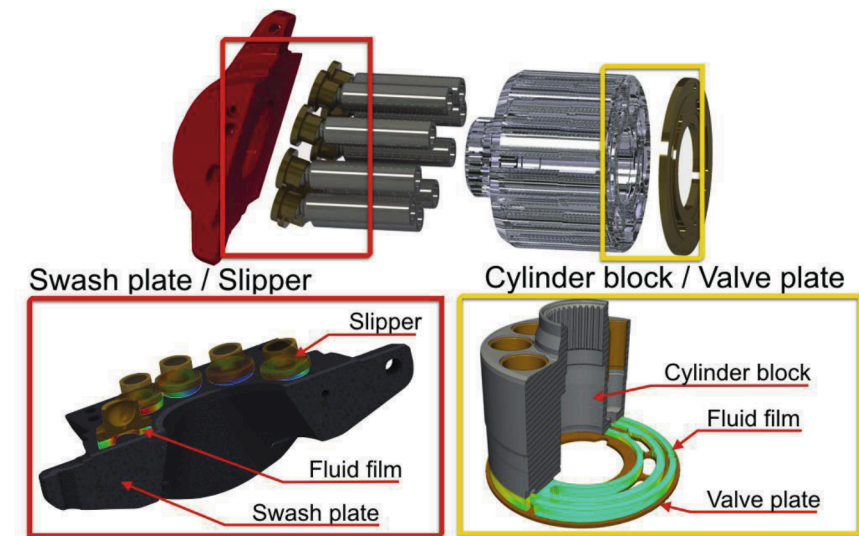


Figure 1 – Studied sealing gaps in the axial piston pump

The measurements will have two purposes, one to measure transient behaviour, and second measure steady state conditions, which can then be used to validate the simulation. The simulation model was used to place the sensors in the appropriate positions, predict problematic operating conditions, and explain observed phenomena. In addition, the measured wear-in behaviour was used to improve the simulation model, by incorporating a simulation based wear prediction [3]. The used test rig set up is shown in Figure 2. The pump's outlet and drain port are equipped with temperature, pressure and particle sensors. The inlet port is also equipped with

temperature and pressure sensors, as well as two filter elements, one fine 4  $\mu\text{m}$  filter as well as a metal filter, which works with permanent magnets. The purpose is to be able to measure the particles generated by the pump itself, without recirculating the particles through the tank. The inlet line is pressure controlled by a supply pump, which guarantees a cavitation free environment, by keeping the pressure at 1.8 bar. The pump is a 92 cc open circuit axial piston pump, rated to 350 bar nominal and 420 bar peak pressures with a maximum speed of 2300 rpm. The test conditions were chosen to be 500-1800 rpm and pressures up to 300 bar. A full list of the measured operating conditions can be seen in the bottom of Figure 5.

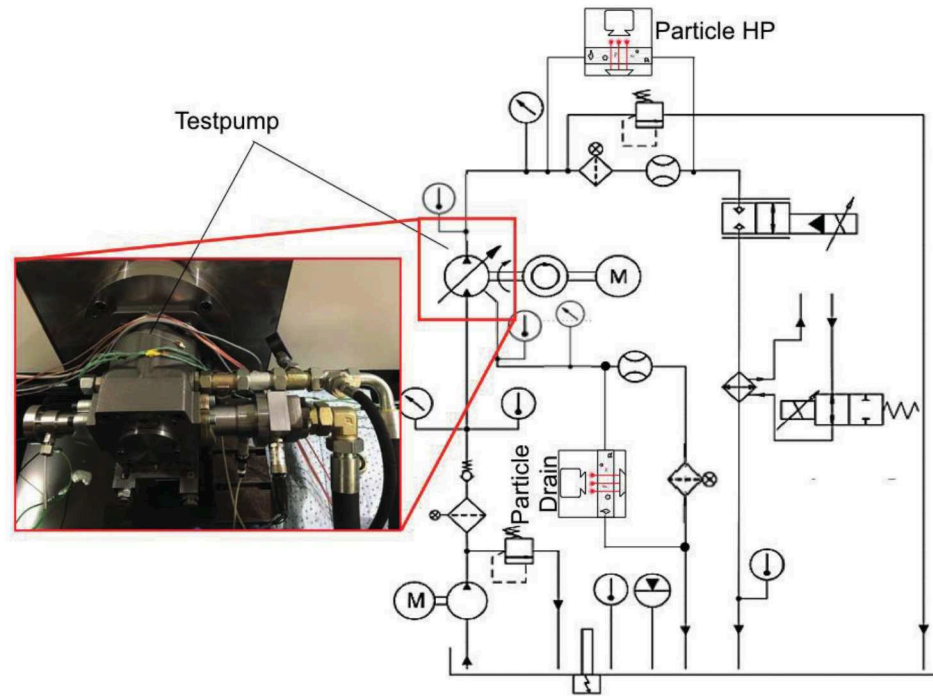


Figure 2 – Test stand “Transparent Pump” schematic

### 3 Prediction of lifetime affecting conditions with respect to temperature

The next section shows the measurements results over various operating conditions. The pump was tested in stationary as well as in transient conditions. In order to reach true stationary conditions, each temperature gradient was zero while the tank temperature was at  $40 \pm 1^\circ\text{C}$ . This took about 30 min per operating condition.

#### 3.1 Measurement set up

A total of eight measurement series were performed. The first four measurement series were focusing on capturing the slipper gap height and swash plate temperature. The slipper measurement set up is shown in Figure 3 on the right. The shown sensor plate (outlined in red) was removable and axis symmetric, therefore there were two positions this plate could be mounted. The first position (oriented as shown in Figure 3) captured the gap heights on the high pressure side, and the second position the gap heights on the low pressure side. Series 1 & 2 were measuring with the sensor plate in position I and the series 3 & 4 in position II. The way the temperature sensors were located, a complete temperature field could only be achieved using data from both plate positions, totalling in 28 unique measurement spots, where some locations were measured in both plate positions in order to compare the measurements.

Series 5 & 6 focused on the temperature measurements on the valve plate only, here no slipper measurements were performed. A total of 26 thermocouples were placed 0.5 mm underneath the running surface at the locations shown in Figure 4 top left. Series 7 and 8 were used to repeat the run-in process for the cylinder block valve plate interfaces. Series 7 used a different run-in pattern (only low pressures), whereas Series 8 repeated the measurement order of Series 5 and 6. In Series 8 both interfaces, slipper / swash plate and cylinder block / valve plate were analysed. Therefore 2 of the 3 main lubricating gaps were measured at the same time, giving a deep look into the pumps performance and being able to estimate the power loss contribution of each interface. An overview of all 8 series can be seen in Table 1.

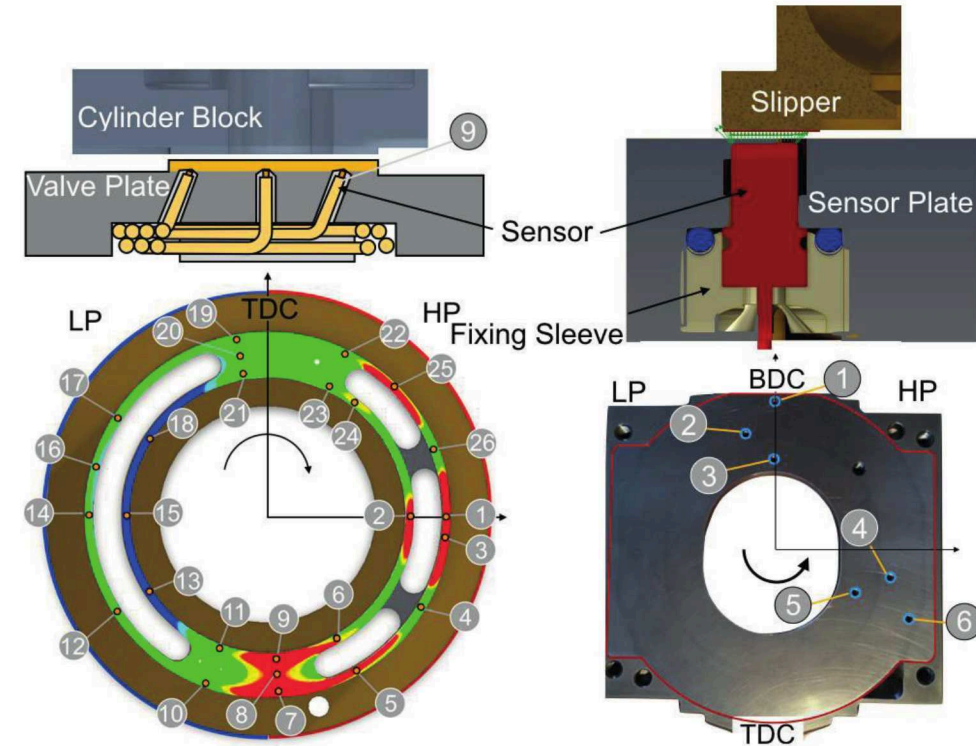


Figure 3 – Sensor instalment for the two interfaces:  
Temperature on valve plate (left), gap sensor swash plate (right)

Table 1 is listing the measured interfaces, the sensors used, as well as the new parts if any were exchanged. It also shows the Swash Plate Position (Position I – gap measurements on the high pressure side and BDC or Position II – gap measurements on the low pressure side and TDC).

In addition, starting at Series 5 particle sensor were placed in the high pressure and drain line as shown in Figure 2. These particle sensors were Argo-Hytos OPCOMII sensors, capable of measuring particles ranging from 4  $\mu\text{m}$  to 21  $\mu\text{m}$  in size. They are mounted in a by-pass configuration and output oil cleanliness and particle concentration in particles/ml. The



Table 1 - Overview of the measurement series

Series	Measured Interface	Swash Plate Position	Measured Sensors in Pump	New Pump parts
1	Slipper / Swash Plate	Position I	6 Eddy Current, 17 Thermocouples (TC)	Everything new, but run-in by the manufacturer, besides the swash plate
2	Slipper / Swash Plate	Position I	6 Eddy Current, 17 TC	N/A
3	Slipper / Swash Plate	Position II	6 Eddy Current, 17 TC	One new slipper
4	Slipper / Swash Plate	Position II	6 Eddy Current, 17 TC	N/A
5	Cylinder Block / Valve Plate	N/A	26 TC, Particle Sensors	New valve plate, new cylinder block
6	Cylinder Block / Valve Plate	N/A	26 TC, Particle Sensors	N/A
7	Cylinder Block / Valve Plate	N/A	26 TC, Particle Sensors	New valve plate. New Block
8	Slipper + Cylinder Block	Position I	6 Eddy Current, 17 + 26 TC, Particle Sensors	New valve plate

Based on the previous publications /9, 10/, it can be concluded that the temperature field captures the gap behaviour in an excellent fashion. Problematic areas are where high temperatures occur, which indicate low fluid film thickness, high viscous friction and low leakage, whereas lower temperatures are due to higher gaps when higher leakage occurs. A sample temperature field for a low speed high pressure applications can be observed in the top of **Figure 4**. Here the temperature field is shown for both interfaces at 300 bar, 500 rpm and 100 % displacement. The swash plate temperature is shown on the top right. It can be seen that there is a region of higher temperature shortly after the transition from low to high pressure (Top Dead Centre – TDC), indicating that in this region the gap height is low. Then there is a region of low temperature at the bottom dead centre (BDC), indicating higher gap heights and higher leakage. The corresponding simulated and measured gap heights are shown in the figure in the middle of Figure 4. The simulated fluid film at  $\phi = 180^\circ$  is shown on the bottom with the three sensor positions. The min and max gap heights are a simulation output, whereas the blue, red and green lines are measured outputs for sensor 1-3 or sensor 5-6 correspondingly.

Similarly, the valve plate temperature, gap height and simulated fluid film is shown on the left side of Figure 4. Here the highest temperatures are around the outer sealing land of on the high pressure side, as well as at both TDC and BDC. On the low pressure side, the gaps are larger and therefore less heat is being generated while more cooling through leakage is introduced. From Figure 4 it becomes clear that the gap height measurements only give a small glimpse at the overall picture, they don't capture the maximum or minimum gap height, rather they output a snapshot of the orientation of the measured part at one instance in time. This is true for both interfaces. The temperature field however delivers a great overview of potentially life time critical conditions.

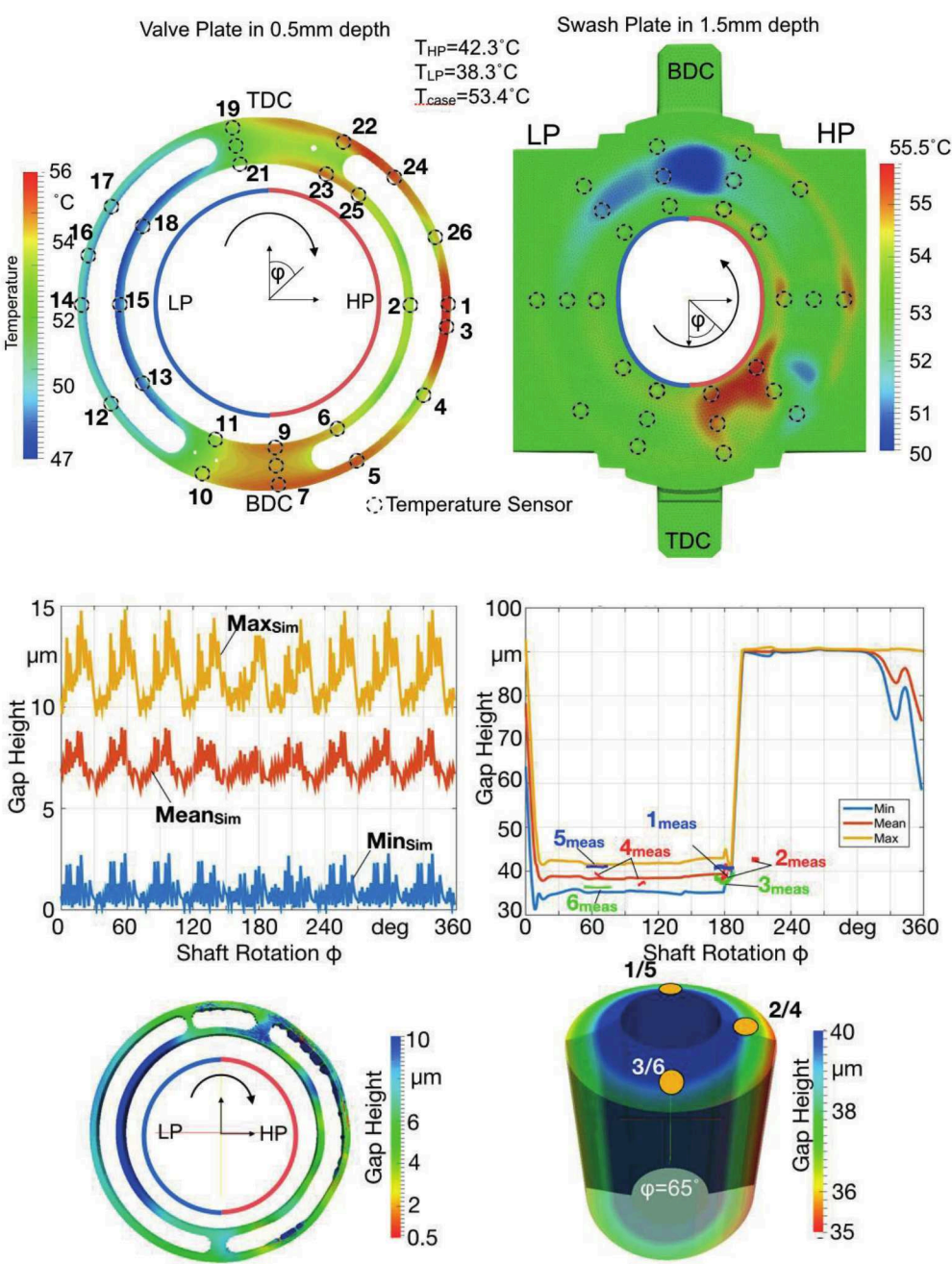


Figure 4 – Example Temperature field (top), measured and simulated gap height (middle) and 3D fluid film (bottom) at 300 bar, 500 rpm and 100% displacement for both interfaces along with the thermocouple placement.

3.2 Steady State Temperature Trends

This section discusses the measured temperature trends, across the entire operating field of the pump. A total of 30 operating conditions were measured in each series, varying pressure, speed and displacement of the pump. Each operating point was held constant until no changes were observed in any of the temperature sensors. The temperatures were then recorded for 2 minutes and averaged over the steadiest period in these 2 minutes. To achieve repeatability between each measurement, the tank temperature was regulated to be 40°C, yielding in roughly 35-38°C inlet temperature, depending on the operating condition. It is also necessary to mention, that the measurements were afterwards adjusted to an inlet of 35°C, to make them comparable to each other. The 30 operating conditions can be seen in the bottom of **Figure 5**. Here the minimum (blue), mean (green), median (black) and maximum (red) valve plate temperatures of the 26 thermocouples are shown across all operating conditions. The shown values are average values from series 5 & 6. It can be observed, that the mean temperature level of the valve plate increases with speed and pressure. The median temperature level is very close to the mean, indicating an evenly distributed temperature field, rather than a few outliers. The effect of the displacement change on the mean temperature level is small, but can be observed. Larger displacements tend to have lower temperature levels than lower displacements. This effect can be explained by rather steady losses but lower volumetric flow, which yields to less cooling of the valve plate. This is confirmed by the fact, that the difference between the min and max temperature stays almost the same when displacement changes occur, indicating that the temperature distribution remained similar, just with a different temperature level. However, there are also other influences on the mean temperature level during the displacement changes besides the change in flow. By taking a look at 500 rpm, 300 bar and 25%, it can be seen that the temperature level is higher than the general trend. Here the influence of the other interfaces can be observed. At this particular point, the slippers generate higher losses (see Figure 6), which increase the case temperature and therefore influences all parts of the rotating kit. Higher case temperature means that the parts such as the valve plate can dissipate less heat towards the surrounding oil, increasing their temperature. This illustrates the complexity of the physical phenomena that occur in these pumps, and how important it is to take all influences into regard when trying to model these gaps.

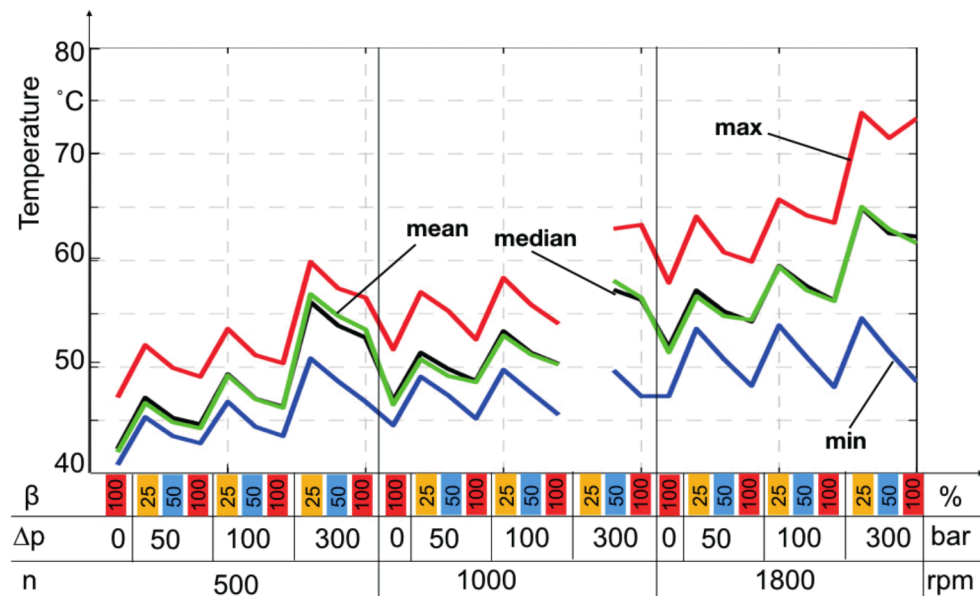


Figure 5 – Min, mean, median and max temperature of the valve plate across 30 operating conditions

Another trend that can be observed in Figure 5, is that the temperature spread, the difference between min and max, increases with pressure but more so with speed. The larger the spread, the higher the thermal strain on the valve plate and the larger the gap height difference.

**Figure 6** shows the temperature distribution of the swash plate in a similar fashion. The shown values are the average of Series 1 - 4. It can be clearly observed, that the trends are different on this interface than on the cylinder block valve plate. What is the same is the general trend that the mean temperature increases with speed, with a few outliers. However, the pressure dependence is different. Medium pressure levels tend to have lower temperatures than higher or lower pressures. The influence of the displacement angle is also not as clear. For some pressure and speed levels the lower displacements have higher temperatures than at higher displacements, but this is not true for all operating conditions.

The spread between min and max varies drastically between operating conditions, with no clear trend visible. The highest spread seems to be at low displacements with a high or low pressures. The missing points for the three 25% displacement operating conditions are due to faulty or incomplete data at these points.

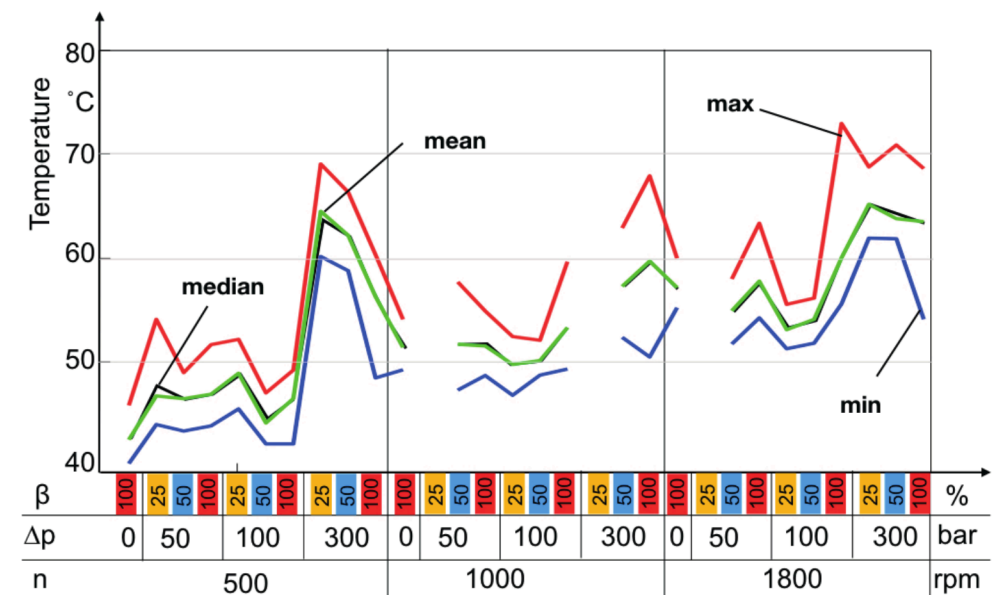


Figure 6 – Min, mean, median and max temperature of the swash plate across 30 operating conditions

In general, these temperature trends can be used to analyse the behaviour of the interfaces at each operating condition. For example, it becomes clear that 500 rpm 300 bar and 25% displacement is a difficult condition for the slippers, while 1800 rpm 300 bar and 100 % displacement is a tough one for the cylinder block / valve plate. Overall the slippers of this pump tend to work better at medium pressure levels.

A different analysis of these temperature trends can be seen in **Figure 7**. Shown on the left is the maximal measured valve plate temperature for varying pressures and speeds at 100% displacement. The grey lines indicate the measured power lines. It becomes obvious that the temperature contour lines are crossing the power lines, which means that the cylinder block valve plate heat generation varies within the same power output. In case of the 20 kW power line for example, the highest point is at 1800 rpm 80 bar with 64°C (purple circle), while the lowest temperature occurs at 750 rpm 200bar with 56°C (green circle), a delta of 8K.



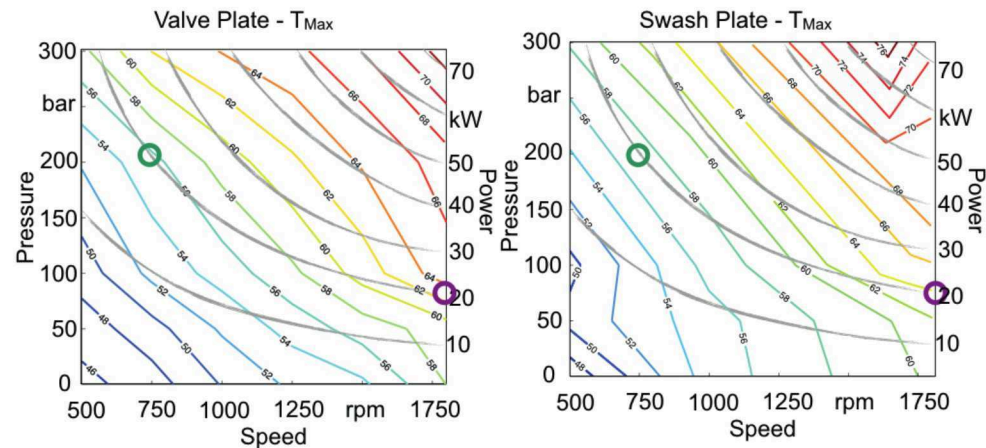


Figure 7 – Max. temperature contour field with measured power lines for both valve plate and swash plate

The right side of Figure 7 shows the maximum temperature on the swash plate also at 100% displacement. The trend is very similar. For example, looking at the 20 kW power line the lowest temperature is at 57°C (green circle) at 200 bar 750 rpm, while the highest is at 64°C (purple circle) at 80 bar and 1800 rpm, yielding a 7 K temperature difference.

Looking at both interfaces, it can be concluded that this particular pump should be operated rather in lower speeds and higher pressures in order to keep the maximum temperatures lower. These shown maximum temperatures were measured at steady state, the transient temperatures were usually higher. Higher hot spots (max temp) usually mean higher viscous friction, which can lead to higher wear. Therefore, if life time extension is desired, lower temperature levels are desirable. For this particular pump, this means running at lower speeds and higher pressures is advantageous.

### 3.3 Transient effects

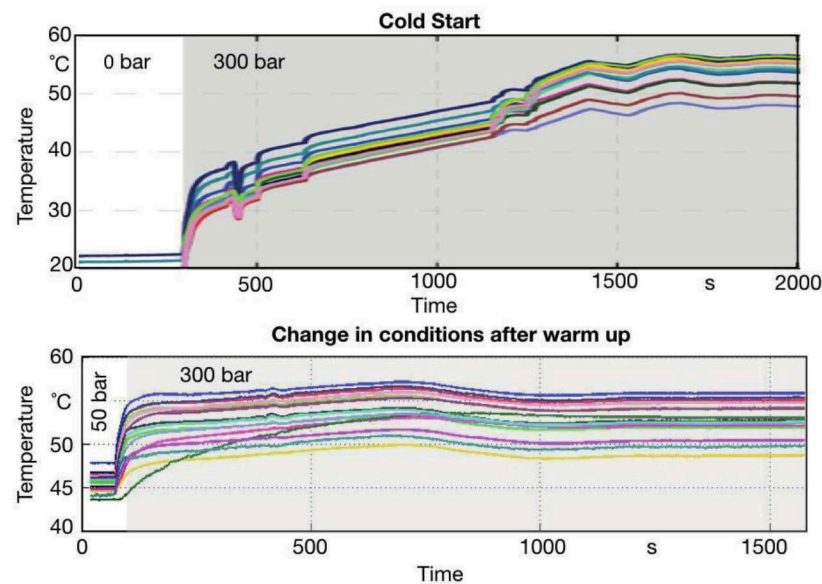


Figure 8 – Transient valve plate temperature for 500 rpm from a cold start and warm transient change

Next to the steady state findings, the transient measurement data gives great insight into dynamic effects such as wear. In contrast to the steady state temperature measurements, during dynamic conditions, such as pressure changes, the pump parts do not have time to heat up or cool off from the previous operating condition. Therefore, it does play a role in which order these measurements have been taken. For the initial run-in phase, the first couple of operating conditions, the order for each series was kept the same. The difference in terms of maximal temperature occurring in the cylinder block / valve plate gap can be seen in **Figure 8**. The upper part of the figure shows a cold start, meaning it's the first operating point of the day, when the oil is still cool. Shown is the pump running at 500 rpm 0 bar with a sudden increase to 300 bar. A steep increase in temperature by roughly 20 K can be observed. The final steady state temperature was reached after 2000 s. Note that the temperature spike during a cold start did never surpass the steady state temperatures. The ups and downs after roughly 1300 s are due to cooling of the tank. The bottom of Figure 8 is the same operating condition, but when the pump is already heated up. The initial spike is lower, however the temperature level is already at or even higher than the steady state level. For this particular operating point the impact of the initial temperature spike doesn't seem too obvious, however during some operating conditions the initial spike is very high, which can indicate wear as shown in the next section.

### 3.4 Wear in behaviour of the valve plate

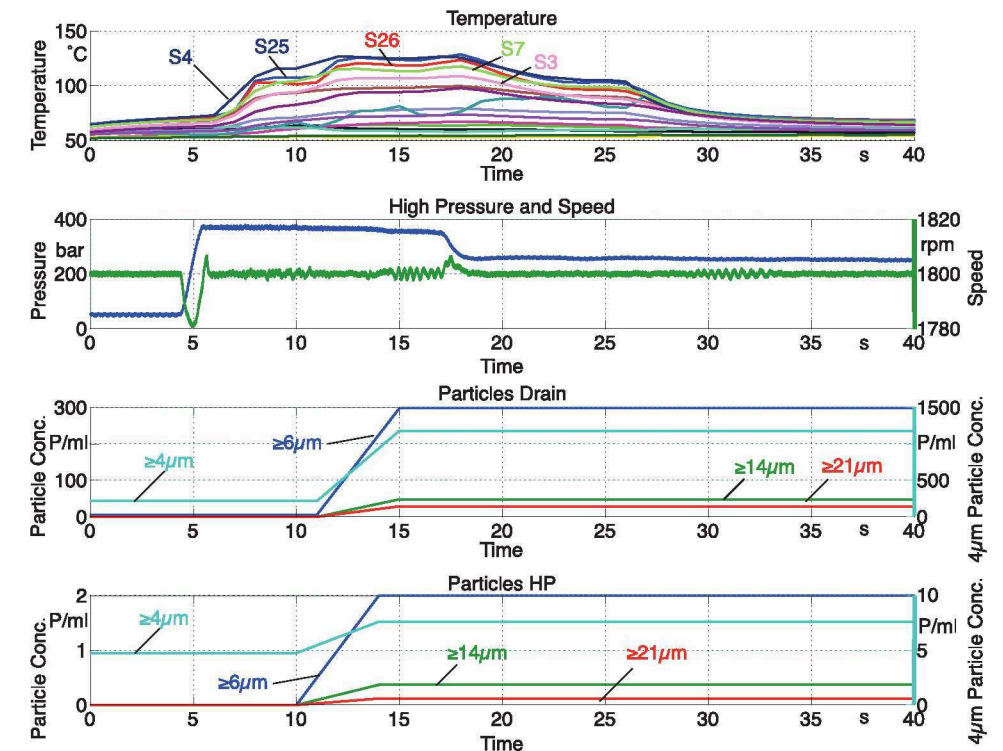


Figure 9 – Valve plate temperature at first time wear in along with particle generation in series 8

**Figure 9** shows the measured transient data for a change in pressure at 500 rpm 100 % displacement, going from 50 to 360 bar. The top figure shows the temperature curves, the one below that the high pressure signal, and the bottom two figures show the data from the particle monitors both in the drain and the high pressure line. They output the particle concentration in parts/ml for four particle sizes:  $\geq 4 \mu\text{m}$ ,  $\geq 6 \mu\text{m}$ ,  $\geq 14 \mu\text{m}$  and  $\geq 21 \mu\text{m}$ . The  $\geq 4 \mu\text{m}$  is shown on the right y-axis due to a different scaling. The important detail here is that both the cylinder block and valve plate have never seen a pressure above 300 bar before this.

The first thing that is quite astonishing, is that temperatures of multiple temperature sensors drastically increased to well above 100°C, as soon as the pressure was increased. After about 12 seconds at this high pressure the pressure was reduced to 300 bar. After that the temperatures dropped again to a normal level. During this period of very high temperature the particles increased drastically in all four particle sizes in both the high pressure and drain line. This behaviour was documented before in this pump and published [9], the resulting temperature curve can be seen in Figure 12 on the left. The previous trend was measured during series 5, when both valve plate and block were new and the pressure was raised to 300 bar for the first time. Unfortunately, during that measurement series the particle monitors were not set up correctly and it was not possible to record the shown particle trend. However, the pump was opened afterwards and the locations that experienced these high temperature levels had significant wear. The above trend in Figure 9 occurred by accident in series 8, it was never planned to increase pressures above 300 bar, however an error in the load valve controller caused this pressure spike. This time the particle sensors were working properly and gave the shown trends.

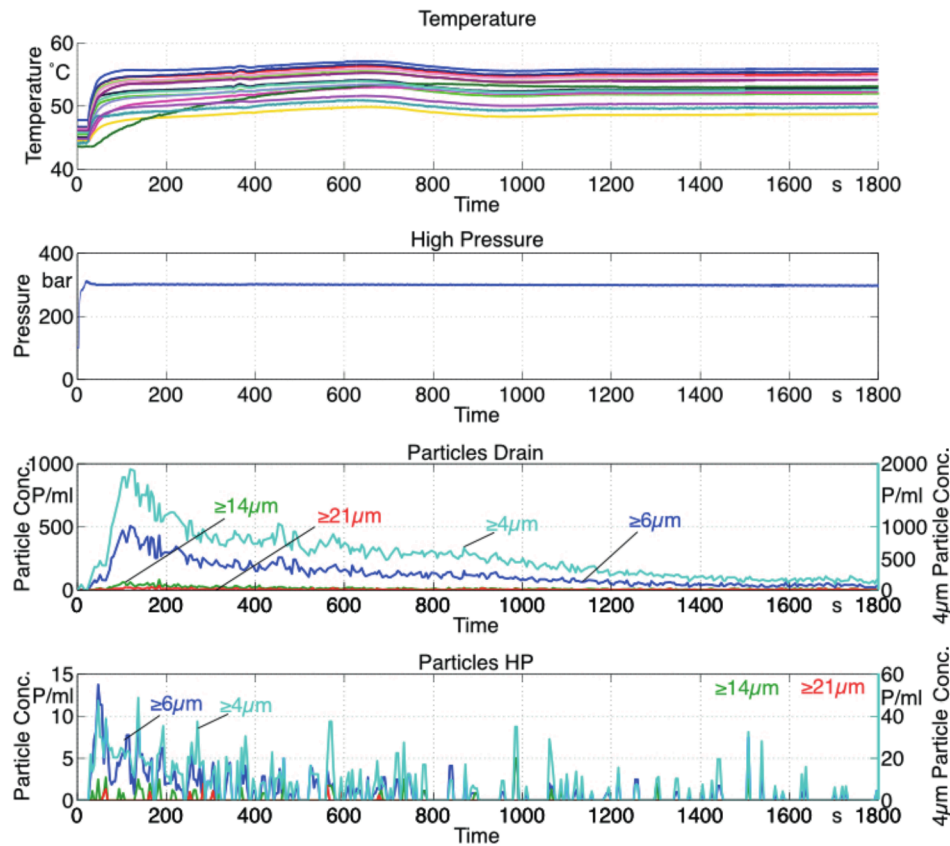


Figure 10 – Wear in temperature in series 8 for valve plate only

The mentioned temperature spike at 300 bar, which occurred during series 5, was not repeatable in series 5 nor 6. This suggested that it was due to a one-time wear-in process. Series 8 had a new valve plate installed, hence it was expected that a similar effect can be observed. The measured valve plate temperature and high pressure as well as drain particle concentration can be seen in Figure 10. Clearly the temperature spike was not nearly as hot as in Figure 9 or the previously published temperature spike, however the particles monitors in both lines clearly saw a large spike, which slowly decreased with time. The particle concentration levels are very comparable to

the ones in Figure 9 and even higher. The fact that there was significant wear but the temperature rise was not above 60°C needs to be further investigated. One theory is that the temperature increase in Figure 9 resulted from both brass and steel wear, where steel wear would only occur at the cylinder block since the valve plate is made from brass. The cylinder block was not replaced for series 8, therefore the cylinder block should be already run-in. Another interesting aspect in Figure 10 is the duration of the particle generation. Even after 1600 s (30 min) and with a steady state temperature level reached, the particle generation has not completely ceased. When the operating point was repeated for a second time in series 8, the particle generation died down significantly, as can be seen in Figure 11.

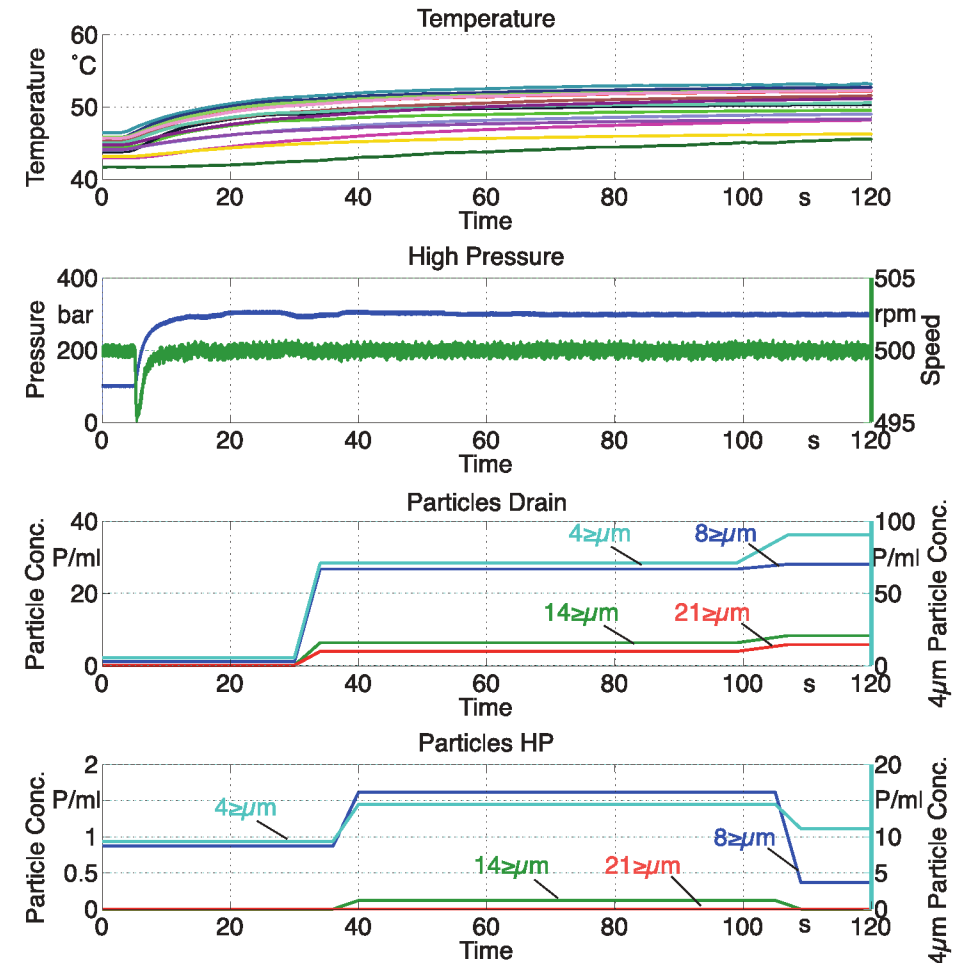


Figure 11 – Valve plate temperature and particle wear for re-rerun of 500 rpm 300 bar 100% in series 8

The initial temperature rise for the re-run is not as high as in the first run (Figure 10), even though the steady state temperature level of the previous operating condition had similar temperature levels. There still is a spike in particle generation, however the concentration levels are much lower than in the first run. A more detailed temperature analysis of the three transient measurements for 500 rpm 300 bar is shown in Figure 12. The figure shows 3 temperature graphs from left to right: The temperature transient temperature for the new valve plate (VP) and new cylinder block (CB) from series 5, the measurement for a new VP from series 8 and the second time the new VP from series 8 experienced the 300 bar. The temperatures are shown for the same time frame,



which makes them more comparable. What becomes obvious is that the temperature levels are different and the sensor that experiences the max. temperature change as well. Above the three graphs is the top 3 max temperature after stationary conditions were reached (adjusted to 35°C inlet). The physical sensor locations are shown in Figure 4 top left.

For the new VP and CB (left graph) the top 3 transient temperature sensors are S5, S7 and S3. After roughly 30 min run-in the max stationary temperature top 3 are: S5, S25 and S3. In series 8 the transient and stationary order changed to: S25, S26 and S4. One outlier is S5 in the right graph, which has here the highest temperature, however this is due to the fact that S5 was the highest in the previous operating condition. Not only the transient temperatures levels are different between the three measurements, but also the final stationary temperature levels, which are decreasing from left to right. The cylinder block is the same for all 3 measurements, therefore it is possible that the more the cylinder block wears-in, the colder the temperatures on the valve plate become.

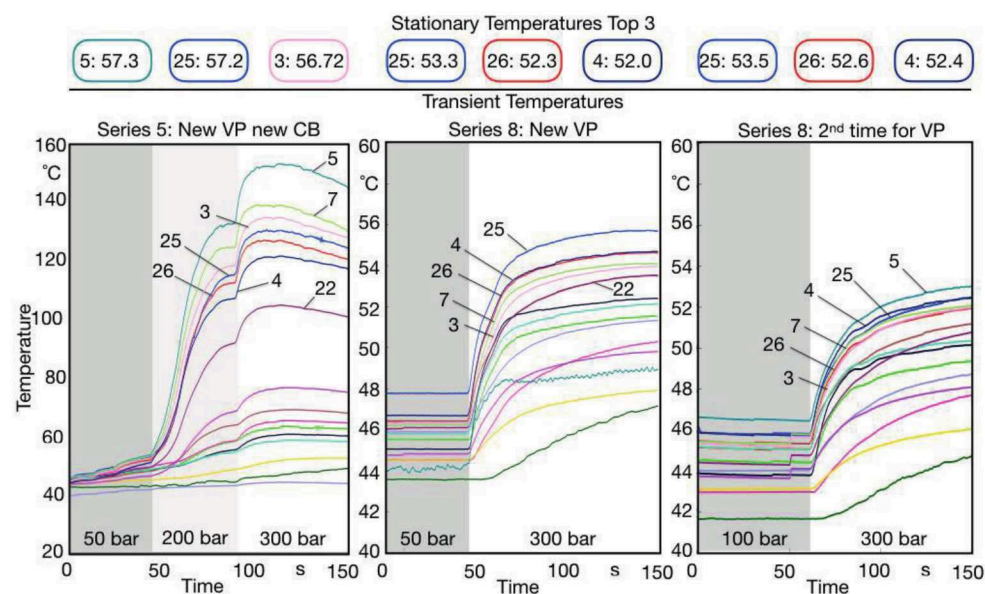


Figure 12 – Transient valve plate temperature rise for 500 rpm 300 bar 100%

Another interesting trend that was noticeable, was that not every operating condition experienced such a strong run-in. It rather seemed that each pressure level independent of speed had to be run-in, as well as every speed level independent of the pressure. For example, after completing the run-in for 500 rpm 300 bar, the effect of increasing the speed to 1800 rpm caused more particle generation, than increasing the pressure from 50-300 bar at the higher speed level. This effect is shown in Figure 13. Here the initial condition is 750 rpm, 50 bar and 100% displacement. Then the speed is increased to 1800 rpm while maintaining the pressure level. After the speed is reached the pressure is increased to 300 bar. This is the first time the valve plate has seen this high speed and high pressure, however the effect on the particle generation by increasing the speed is larger than the pressure increase.

An overview of the max particle concentration for each of the four shown cases, can be seen in Figure 14. The two bar charts show the max. recorded particle concentration for the different particle sizes. The blue bar represents the first time the new valve plate in series 8 has experienced 300 bar. The green bars show the max particles for the second time the valve plate experienced 300 bar in series 8. The orange shows the 360 bar case (first for both valve plate and cylinder block see Figure 9) The red bars show the additional particle concentration caused by the pressure increase from 50-300 bar at 1800 rpm as seen in Figure 13. The trend

shown is that the particle generation drastically decreases after the first time the pump parts have experienced a new pressure level. This is true even if the speed changes.

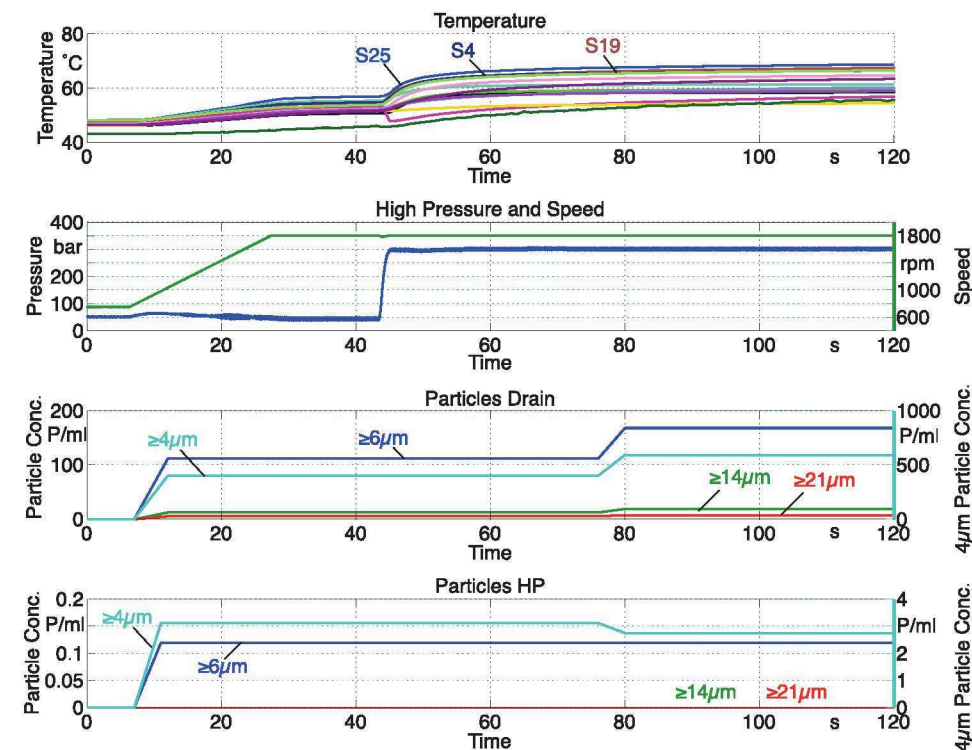


Figure 13 – Valve plate temperature and particles for speed and pressure change – first 300 bar pressure at high speed

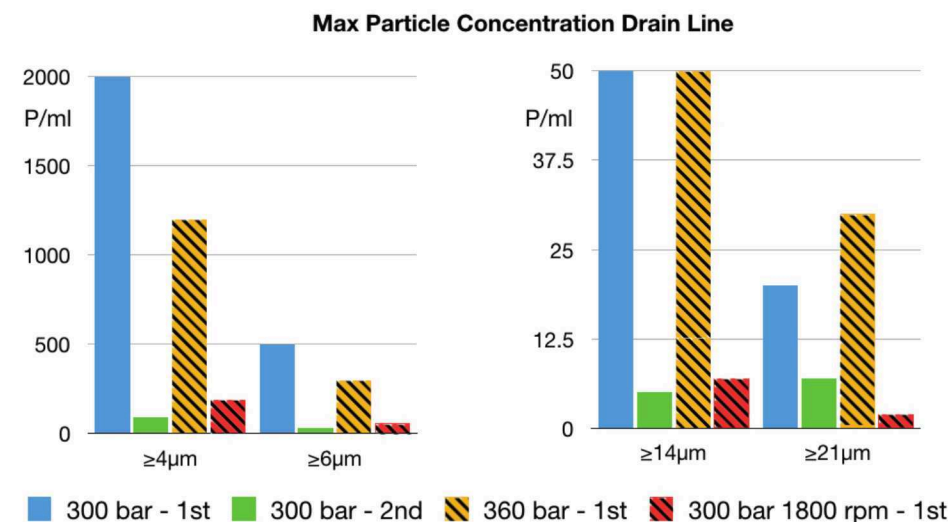


Figure 14 – Overview max. particle concentration for 500 rpm 100 % displacement.

To conclude, it can be said that a run-in occurs every time the pump either experiences a never-before seen pressure or speed level. However, the two can be seen independently from each other. The pump run-in can take about 30 min per operating condition for the cylinder block valve plate interface. A direct connection between temperature rise and particle generation can be seen, but cannot be quantified at this point, since a similar particle generation caused two different transient temperature curves.

#### 4 Summary and Conclusion

This paper presented both transient and steady state measurement from a novel “transparent pump” test rig. The measurements included surface temperature measurements of the valve plate, swash plate as well as the fluid film thickness of the slipper. Combined with particle sensors the data was used to analyse wear patterns and the run-in of the valve plate interfaces. A state of the art simulation program was used to analyse the pump and interpret the measured data. Especially the gap height measurements are greatly enhanced when combining them with the simulation findings.

The novel findings are that changes in pressure and speed have significant impact on the valve plate surface temperatures, whereas changes in displacement are rather insignificant. The surface temperature of the swash plate has a similar speed dependency; however, the slippers react differently to pressure or displacement changes than the cylinder block. Medium pressures tend to have lower temperatures than very high or low pressures. It was also shown that the CB/VP interface can be influenced by the other interfaces, by being affected of elevated case temperatures, which were caused by increased slipper losses. Figure 7 illustrated that the examined pump operates at lower temperature levels at low speed and higher pressure for both the slipper/swash plate and CB/VP interface.

It was also shown that the run-in of the cylinder block and valve plate are accompanied by temperature changes in the transient regime. It was also shown that the run-in is not always the same and is influence by other factors that need to be studied in more detail. A typical run-in phase was about 30 min, after that time the particle generation was significantly reduced.

The next steps in this research are to show the slipper wear and its effect on the performance of the slipper / swash plate interface. The fluid film measurements of the cylinder block / valve plate will be published in future publications. The slippers experience a much longer run-in period than the cylinder block. Furthermore, the simulation tool will be further enhanced by incorporating the wear-in, something that showed already tremendous potential for the cylinder block / valve plate interface.

#### 5 Acknowledgements

This research was funded by the German Federal Ministry of Economic Affairs and Energy (Ref. No. 03SX382B). The authors are responsible for the content of this publication.

Special thanks to Argo-Hytos and Micro-Epsilon for their support of this research with their donation of measurement equipment.

#### Nomenclature

Variable	Description	Unit
$\beta$	Pump Displacement	[%]
BDC	Bottom Dead Centre	

CB	Cylinder Block	
$\Delta p$	Difference between High and Low Pressure	[bar]
HP	High Pressure	[bar]
LP	Low Pressure	[bar]
n	Rotational Speed	[rpm]
$\phi$	Shaft Rotational Angle	[°]
T <sub>Case</sub>	Temperature in Drain Line	[°C]
T <sub>HP</sub>	Temperature in High Pressure Line	[°C]
T <sub>LP</sub>	Temperature in Low Pressure Line	[°C]
T <sub>Max</sub>	Maximum Temperature	[°C]
TC	Thermocouple	
TDC	Top Dead Centre	
VP	Valve Plate	

#### References

- /1/ IVANTYSYNOVA, MONIKA: *An investigation of viscous flow in lubricating gaps*, SVST Bratislava, Czechoslovakia, 1983
- /2/ WERNECKE, P.W.: *Messung physikalischer Größen im Dichtspalt*. In: o+p ölhydraulik und pneumatik (1982), Nr. 26
- /3/ WINNER, D.: *Verschleißempfindlichkeit von verschiedenen Verdrängereinheiten*. In: o+p ölhydraulik und pneumatik Bd. 28 (1984), Nr. 4
- /4/ DEEKEN, MICHAEL: *Simulation of the tribological contacts in an axial piston machine*. In: IMECE04, 2004, S. 1–5
- /5/ PELOSI, MATTEO: *An Investigation on the Fluid-Structure Interaction of Piston/Cylinder Interface*, Purdue University, 2012
- /6/ SCHENK, ANDREW: *Predicting Lubrication Performance Between the Slipper and Swashplate in Axial Piston Hydraulic Machines*, Purdue University, 2014.
- /7/ ZECCHI, MARCO: *A novel fluid structure interaction and thermal model to predict the cylinder block/valve plate interface performance in swash plate type axial piston machines*, Purdue University, West Lafayette, IN, 2013
- /8/ WEGNER, STEPHAN: *Experimental investigation of the cylinder block movement in an axial piston machine*. In: FPMC2015 -9529, 2015
- /9/ IVANTYSYN, ROMAN ; SHORBAGY, AHMED: *An Approach to Visualize Lifetime Limiting Factors in the Cylinder block / Valve Plate Gap in Axial Piston Pumps*. In: FPMC2017-4327, 2017, S. 1–12
- /10/ IVANTYSYN, ROMAN ; WEBER, JÜRGEN: *“Transparent Pump” – An approach to visualize lifetime limiting factors in axial piston pumps*. In: ASME 2016 9th FPNI Ph.D Symposium on Fluid Power. Florianapolis, Brazil, 2016
- /11/ BERGADA, J. M. ; DAVIES, D. L. ; KUMAR, S. ; WATTON, J.: *The effect of oil pressure and temperature on barrel film thickness and barrel dynamics of an axial piston pump*. In: Meccanica Bd. 47 (2012), Nr. 3, S. 639–654
- /12/ KIM, JONG-KI ; JAE-YOUN, JUNG: *Measurement of Fluid Film Thickness on the Valve Plate in Oil Hydraulic Axial Piston Pumps (Part I)* Bd. 17 (2003), Nr. 2, S. 246–253 — ISBN 8263270391

